Noise and oscillatory zoning of minerals

Article *in* Geochimica et Cosmochimica Acta · June 2000

DOI: 10.1016/S0016-7037(99)00444-5

CITATIONS
70

READS
239

3 authors:

Terje Holten
Petromarker
20 PUBLICATIONS **254** CITATIONS
SEE PROFILE

Bjorn Jamtveit
University of Oslo
190 PUBLICATIONS **8,322** CITATIONS
SEE PROFILE

Paul Meakin
Temple University
515 PUBLICATIONS **27,509** CITATIONS
SEE PROFILE

Pergamon

Geochimica et Cosmochimica Acta, Vol. 64, No. 11, pp. 1893–1904, 2000

0016-7037/00 $20.00 + .00

PI S0016-7037(00)00444-5

Noise and oscillatory zoning of minerals

TERJE HOLTEN,* BJØRN JAMTVEIT, and PAUL MEAKIN

Fluid-Rock Interactions Group, Departments of Geology and Physics, University of Oslo, P.O. Box 1047 Blindern, N-0316 Oslo, Norway

(*Received March* 8, 1999; *accepted in revised form December* 16, 1999)

Abstract—Oscillatory mineral zonation is usually associated with crystal growth in an open system, either a hydrothermal system or a melt after a period of magma mixing or degassing. Such systems may be driven sufficiently far from thermodynamic equilibrium to produce autonomous patterns by geochemical self-organization. The resulting zonation patterns will be the result of coupling between the generally nonlinear crystal growth dynamics and the boundary conditions imposed by externally controlled fluctuations. We examine the effects of noisy boundary conditions on four different crystal growth models. These are models for plagioclase growth in magmatic systems (L'Heureux and Fowler, 1996), for carbonates in sedimentary systems (Wang and Merino, 1992), for garnets in hydrothermal systems (Jamtveit, 1991), and for silicate growth from a melt (Wang and Wu, 1995). The plagioclase model is sensitive to noise, even to low amplitude noise, implying that an observed zonation pattern will be significantly affected by processes other than local growth and transport processes. For the garnet model, fluctuations in the external environment may cause synchronization, so that different crystals develop similar zonation patterns, even if the formation of zonation patterns is a consequence of nonlinear local dynamics. This implies that similarity in intracrystalline zonation does not necessarily imply that the zonation pattern was produced by changes in the external (environmental) conditions. The formation of a zonation pattern may be a consequence of local nonlinearities in the growth process, but the pattern details may be strongly affected by subtle changes in the external environment. *Copyright © 2000 Elsevier Science Ltd*

1. INTRODUCTION

During recent decades, interest in pattern formation in geological systems has grown substantially. Both simple and complex patterns may be created by spontaneous autonomous processes reflecting the nonlinear dynamics of a system far from equilibrium (e.g., Merino, 1984, 1987; Ortoleva, 1994; Jamtveit and Meakin, 1999). However, geological materials and systems are generally heterogeneous and subject to complicated boundary conditions. Consequently, an observed pattern may be a direct consequence of spatial and temporal fluctuations in the environment in which it is formed. In general, both internal autonomous processes and changing external conditions will influence pattern formation, and the interplay between these two types of processes may lead to surprising results. Oscillatory intracrystalline mineral zonation or chemical banding within single crystals is an extensively studied example of geological pattern formation (Shore and Fowler, 1996). Oscillatory zonation can also be produced in synthetic samples (Putnis et al., 1992; Reeder et al., 1990). It may arise in magmatic, metamorphic, and sedimentary settings, but it almost invariably occurs in an open system, with a continuous or discontinuous mass flux into or through the region in which crystal growth takes place. Thus, the growing volume of literature discussing the origin of such zonation has elaborated on external versus internal controls on the observed patterns. Because an open system is often characterized by both complicated boundary conditions (due to phenomena such as variations in fluid flux and composition, magma mixing, and degassing processes) and nonequilibrium states, the coupling of external and internal processes needs to be analyzed. Neither the growth dynamics nor the energetics of processes leading to oscillatory zonation are understood in detail. Insight can be gained by studying the sensitivity of existing crystal growth models to noisy boundary conditions in various regions of their parameter spaces. The nonlinear models that were the basis for the work reported here were developed to gain insight into the origins of oscillatory zoning of plagioclase in magmatic systems (L'Heureux and Fowler, 1996a), carbonates in sedimentary systems (Wang and Merino, 1992), garnets in hydrothermal systems (Jamtveit, 1991), and silicate growth from a melt (Wang and Wu, 1995). The motivation for this work was to explore the effects on zonation patterns of fluctuations in the composition of the fluids or melts from which minerals are growing, with the objective of bridging the gap between patterns produced by existing models and observed zoning patterns. It turns out that for some models even low amplitude noise at the boundaries may significantly affect the observed zonation patterns in some regions of their parameter spaces. This sensitivity to fluctuations in the boundary conditions may also explain why observed zonation patterns can rarely be explained or reproduced statistically by simple autonomous deterministic models.

1.1. Self-Affine Noise

It has recently been shown that some oscillatory zoning patterns can be described in terms of fractal geometry over more than two decades of length scale (Halden and Hawthorne, 1993; Holten et al., 1997). A fractal is an object for which the structure remains the same (or the statistical measures describing the structure remain unchanged) when it is examined on different scales. In recent years, fractal geometry has been used

* Author to whom correspondence should be addressed (terje.hol@geologi.uiO.no).

to describe a wide range of phenomena in quantitative terms (Mandelbrot, 1982; Meakin, 1998). A fractal that is invariant under isotropic dilation or contraction is said to be self-similar. A fractal that has different scaling properties in different directions is self-affine. A self-affine fractal must be magnified by different amounts in different directions to "look the same." The Brownian process $B(t)$ that describes the distance moved after a time t by a particle undergoing Brownian motion from its position at time $t = 0$ is a familiar example of a self-affine fractal. The Brownian process is (statistically) invariant to transformations that change the time scale by a factor of λ and simultaneously change the distance scale by a factor of $\lambda^{1/2}$. This scaling symmetry can be represented by the equation

$$B(\lambda t) \equiv \lambda^{1/2} B(t) \tag{1}$$

or

$$\lambda^{-1/2} B(\lambda t) \equiv B(t), \tag{2}$$

where "$\equiv$" means statistically equivalent to (all of the statistical measures used to characterize the Brownian process and the rescaled Brownian process $\lambda^{-1/2}B(\lambda t)$ are the same). An important example of a self-affine fractal is the surface of the Earth, which can be described by the scaling relationship

$$\langle |\delta h(\lambda x)| \rangle = \lambda^H \langle |\delta h(x)| \rangle, \tag{3}$$

where $\delta h(x)$ is the height difference between a pair of points on the surface of the Earth that are separated by a horizontal distance of x. Most studies of the Earth's topography indicate that the exponent H has a value that is greater than 1/2 and smaller than 1 (values close to 0.75 are the most commonly reported). In a self-affine zoning pattern, the absolute magnitude of the composition difference (or the difference in some quantity related to the composition) $|\delta y|$ between pairs of points separated by a distance δx in the x-direction (the growth direction) scales on the average as $\langle |\delta y| \rangle \sim (\delta x)^H$ (where $\langle \ldots \rangle$ indicates an average). The exponent in this relationship and in Eqn. (1) is called the Hurst exponent. A Hurst exponent (H) greater than 0.5 indicates that the function $y(x)$ is persistent. This means that an increase in y as x is increased is more likely to be followed by an additional increase in y if x is increased further than by a decrease in y. The correlations between the increments in y ($\delta y(x) = y(x + \delta x) - y(x)$) are long ranged ($\langle \delta y(x_0) \delta y(x_0 + x) \rangle$ decays only as a power of x). In the case of a time record, an increasing trend in the past favors an increasing trend in the future (and vice versa). If $H < 0.5$, the record is antipersistent, and an increasing trend in the past favors a decreasing trend in the future. Many different methods have been used to measure Hurst exponents. In the case of single-valued functions $y(x)$, measurement of the dependence of the width $w(l)$ of the function $y(x)$ on the interval l in x over which the width is measured is a common approach (Meakin, 1998). The width $w(l)$ can be defined as

$$w(l) = [\langle y^2(x) \rangle_l - \langle y(x) \rangle_l^2]^{1/2}, \tag{4}$$

where $\langle \ldots \rangle_l$ denotes an average over all sections (x_0 to $x_0 + l$) of length l. If the function $y(x)$ is self-affine, the width w scales as

$$w(l) \sim l^H. \tag{5}$$

Zoning patterns cannot be self-affine on arbitrarily long length scales, because the concentration range Δc of a particular chemical component (the difference between maximum and minimum concentration) is bounded. This implies that the concentration profile might be self-affine on short length scales, but on sufficiently long length scales, an effective Hurst exponent close to zero will be measured. The crossover from the short length scale self-affine behavior to the long length scale nonfractal behavior can be described by the scaling form

$$w(l) = l^H f(l/l^*), \tag{6}$$

where l^* is the characteristic crossover length. The scaling function $f(x)$ is given by

$$f(x) = \begin{cases} c' & x \ll 1 \\ c' x^{-H} & x \gg 1, \end{cases} \tag{7}$$

where $c' \simeq (l^*)^{-H} \Delta c$ is a constant (Holten et al., 1997).

1.2. Nonlinear Systems, Chaos, and Noise

Simple nonlinear systems may exhibit surprisingly complex behavior. Extreme sensitivity to initial conditions is characteristic of a wide variety of nonlinear systems (Lorenz, 1963; Strogatz, 1994; Scott, 1991), and such systems are called chaotic. After an initial transient the system evolves toward a set of points or an asymptotic trajectory called the attractor, which is a fractal for chaotic systems. The attractor can be enclosed inside a finite volume. Often a dynamical model is chaotic in some regions of its parameter space, and periodic or stable in other parts.

If $\mathbf{x}(0)$ is a point on the attractor at time $t = 0$ and $\mathbf{x}(0) + \delta(0)$ is a neighboring point separated initially by an infinitesimal distance $\delta\mathbf{x}(0)$; ($\|\delta\mathbf{x}(0)\| \to 0$), then, in a wide range of numerical studies of nonlinear systems, it is found that the separation between the two points increases exponentially with increasing time t. This exponential increase can be represented by

$$\|\delta x(t)\| \sim \|\delta x(0)\| e^{\lambda t}, \tag{8}$$

where λ is called the Lyapunov exponent (Strogatz, 1994) ($\|\ldots\|$ means scalar or absolute value). A positive Lyapunov exponent means large sensitivity to noise, while a negative exponent means low or no sensitivity. This equation is valid only in an average sense and for a limited time, because $\delta\mathbf{x}(t)$ must be much smaller than the size of the attractor itself. In general, there may be several different Lyapunov exponents corresponding to different directions in the phase space. Usually, only the highest exponent is of interest, since it dominates the overall behavior after a certain time. There has been little research on Lyapunov exponents in systems described by one or more partial differential equations. In particular, the conditions under which Eqn. (8) is valid are not well understood.

Kantz (1994) has provided a reliable method for estimating the maximum Lyapunov exponent. A variation of this method was independently published by Rosenstein et al. (1993). The maximum Lyapunov exponent can be determined by using several trajectories or just one trajectory; here only one trajectory is used. The method consists of finding all points $\mathbf{x}(t_i)$ in a time series that are within a distance ϵ from the reference point $\mathbf{x}(t)$ at time t. The distance between the points $\mathbf{x}(t_i + \overset{*}{\tau})$ and $\mathbf{x}(t + \overset{*}{\tau})$ is

$$d_i(t,\overset{*}{\tau}) = \|\mathrm{x}(t_i + \overset{*}{\tau}) - \mathrm{x}(t + \overset{*}{\tau})\|, \quad (9)$$

where $\overset{*}{\tau}$ is the time increment. The region in space containing points within a distance less than ϵ (the ϵ-neighborhood) is denoted U_t and its volume is Z. Rearranging Eqn. (8), the largest Lyapunov exponent can be estimated as

$$\lambda = \frac{1}{\overset{*}{\tau}} 1\mathrm{n} \frac{\|\mathrm{x}(t_i + \overset{*}{\tau}) - \mathrm{x}(t + \overset{*}{\tau})\|}{\|\mathrm{x}(t_i) - \mathrm{x}(t)\|} \quad (10)$$

This procedure is repeated for each point $i \in U_t$ inside the ϵ-neighborhood and each point $\mathbf{x}(t) = \mathbf{x}\,(n\delta t)$ in the time series, where δt is the time step and n is a positive integer, and the results are averaged. The effective largest Lyapunov exponent is then given by $\lambda = dS(\overset{*}{\tau})/d\overset{*}{\tau}$, where

$$S(\overset{*}{\tau}) = \frac{1}{N} \sum_{n=1}^{N} 1\mathrm{n}\left(\frac{1}{Z} \sum_{i \epsilon U_t} d_i\,(n\delta t, \overset{*}{\tau}) \right) \quad (11)$$

and N is the number of starting times, which should be as large as possible. Often the initial transient is not used for estimating λ, so that the first sum in Eqn. (11) starts with $n > 1$.

Synchronization is an important aspect of the effects of noise on dynamical systems. If two systems with different initial states A and B and the same internal dynamics, characterized by one or more positive Lyapunov exponents, are subjected to the same noise or perturbation they are said to be synchronized if they converge toward and remain in the same state (Gutiérrez and Iglesias, 1998; Malescio, 1996; Pecora and Carroll, 1990). A model can show synchronization in parts of the parameter space, but not in other parts. The synchronization depends on the amplitude of the noise. If the noise amplitude is too low, a system that synchronizes with a high noise amplitude may never synchronize. Pecora and Carroll (1990) were the first to describe synchronization. They defined the "conditional Lyapunov exponents" or sub-Lyapunov exponents, which are the Lyapunov exponent for certain subsystems of chaotic systems. According to Pecora and Carroll (1990) synchronization occurs for the subsystem variables if the conditional Lyapunov exponents (the Lyapunov exponents for the subsystem) are all negative. However, some systems can become synchronized even if one or more of the conditional Lyapunov exponents is positive (Gutièrrez and Iglesias, 1998; Maritan and Banavar; 1994). A third variant of synchronization is phase synchronization (or phase locking). This can be defined as the appearance of a certain relation between the phases of interacting systems (or between the phase of a system and that of an external force), while the amplitudes are, in general, not strongly influenced by the interaction (Pikovsky et al., 1997). However, the notion of phase and amplitude in chaotic systems is non-trivial. A fourth variant of synchronization is partial synchronization (Hasler et al., 1998). This term is used to describe systems in which only some of the state variables synchronize and the others do not synchronize with them.

2. RESULTS

In this section, the results of an investigation of the effects of noise on four nonlinear models for oscillatory zoning are described. Many phenomena associated with these models can occur in systems other than those that they were developed to represent. When a system is subjected to random noise, the noise will be amplified or dampened, depending on the sign of the Lyapunov exponent. The coupling between noise and nonlinearity leads to interesting phenomena such as sensitivity to noise, noise-induced transitions, synchronization, desynchronization, and stochastic resonance.

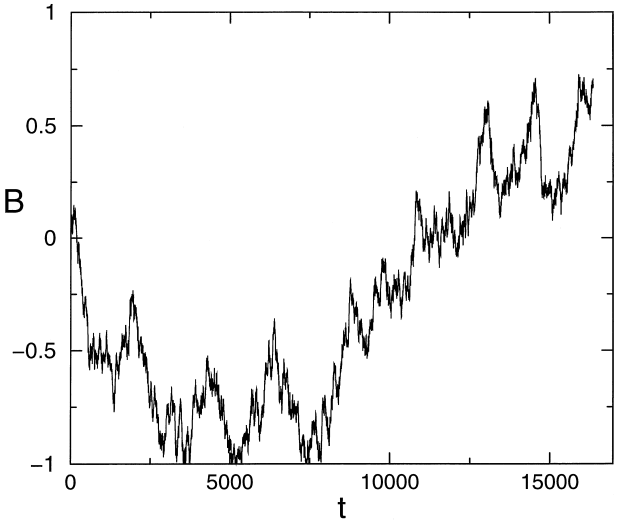

Fig. 1. Bounded Brownian motion with a Hurst exponent of 0.5 generated using the second method described in the text. The curve starts at $B = 0$ and there are 16384 time steps.

2.1. Bounded Noise

Mineral zoning patterns are always bounded, because the molar fractions must lie in the range 0 to 1, and the compositions of the solutions or melts from which they grow are bounded in a similar manner. In practice, the molar fractions are often much more severely bounded. There are many ways to construct a bounded self-affine fractal. One approach is to scale the fractal after it has been generated. The second method to create a bounded self-affine fractal is to randomly draw a number from a Gaussian distribution with a zero mean and add it to the current value, B. If the new value of B lies outside of the permissible limits, a new Gaussian random number is generated and added to B until the new value of B is within the limits. This method was used throughout this article. If the Gaussian increments are correlated, fractals with $H \neq ½$ can be obtained. An example of such bounded Brownian noise is shown in Figure 1. Unless otherwise stated, this is the input noise for all models in this article that contain noise. A third method is analogous to the movement of a particle in a potential E (y). First, a noisy self-affine fractal $B(t)$ without bounds is created. The successive increments $\delta y = \delta B = B\,(t + \delta t) - B(t)$ in this noise are then used to generate trial moves for the particle. If the increment δy moves the particle to a lower potential, the step is always taken (t is increased by δt and $y(t + \delta t) = y(t) + \delta y$) and if the increment is upwards in potential, the step is taken with a probability $p = \exp((E_1 - E_2)/kT)$, where E_2 ($E[y(t + \delta t)]$) is the new potential value and E_1 ($E[y(t)]$) is the old potential value, k is the Boltzmann constant, and T is the temperature. Depending on the potential and the

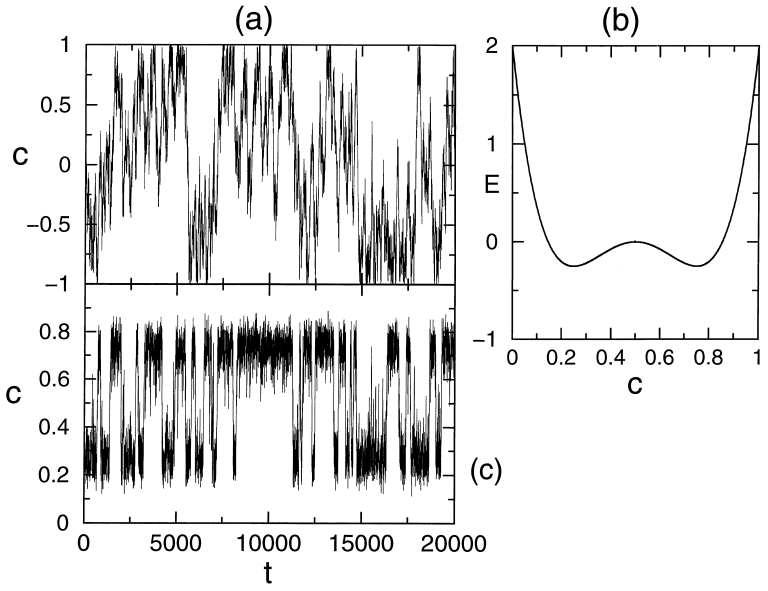

Fig. 2. (a) Brownian noise. (b) The potential E in Eqn. 12 as a function of composition c. (c) The concentration c as a function of time t generated using the method described in the text with the increments used to generate part (a), the potential shown in part (b) and $kT = 0.1$. In this example, 20000 time steps (increments) were used.

temperature, different features are observed. The most simple procedure is to use a simple quadratic $E(y) = A(y - y_0)^2$ or quartic $E(y) = A(y - y_0)^4$ potential. This procedure can be used to obtain concentration records $c(t)$ with bounded fluctuations, by using a concentration potential $E(c)$. More complex potentials can be used to obtain a more realistic representation of the concentration fluctuations in natural systems. For example, potentials with two minima, like the dimensionless potential

$$E(c) = \frac{(4c - 2)^4}{4} - \frac{(4c - 2)^2}{2}, \qquad (12)$$

where c is the concentration, can be used. This potential is plotted in Figure 2b. It has minima at (¼, − ¼) and (¾, − ¼) and a local maximum at (½, 0). If the temperature is low, the output signal will fluctuate about one of the minima. At intermediate temperatures, the output signal will fluctuate about one minimum and then jump to the other minimum, from time to time. At high temperatures, only the quartic part of the potential will influence the concentration fluctuations. An example of such noise-induced transitions is shown in Figure 2c. The output function fluctuates about the two minima. In this example, the fluctuations are quite large. The potential has the effect of limiting the effective concentration range Δc. At all temperatures, the noise generated by this procedure will be similar to the input noise (with the same Hurst exponent) on small time scales. However, there will be a crossover from the short time scale unbounded noise to the long time scale bounded noise with a Hurst exponent of 0. In the case of complex potentials, the crossover may be complex and may extend over a number of decades (depending on the temperature). Under these circumstances, the dependence of the width (rms amplitude fluctuations) of the noise on the interval over which it is measured may exhibit an approximate power law behavior that might be incorrectly interpreted as an intermediate self-affine scaling regime. This method of generating bounded noise may be used as a model for the external concentration fluctuations (the noise) during crystal growth.

2.2. Noise Signals With Periodic Components

A question that is important in the interpretation of log-log plots is how periodic components superimposed on a self-affine function affect the interpretation. It is likely that many natural zonation patterns consist of both periodic components and noise without any distinct frequencies (like fractal noise). Figure 3a shows the width function $w(l)$ obtained by analyzing a periodic component added to a Brownian process noise signal. At time scales below the period of the periodic component, the effective Hurst exponent is increased. At longer time scales, the effective Hurst exponent is decreased. Even a small periodic component has a significant effect on the effective Hurst exponent. The crossover occurs over a range of time scales that include the period of the periodic component, t_p. If t_p is small, most of the observed part of the curve will have an artificially lowered effective Hurst exponent.

2.3 Plagioclase Growth Model

The most convincing indication of autonomously produced oscillatory zonation is probably shown by plagioclase, since the composition within a single grain can change significantly over micrometer scales (Pearce and Kolisnik, 1990). Models for plagioclase growth have been reviewed by Pearce (1994). L'Heureux (1993) and L'Heureux and Fowler (1994) studied a model for plagioclase growth that is based on isothermal crystallization from a melt in an open system. The growth equation is

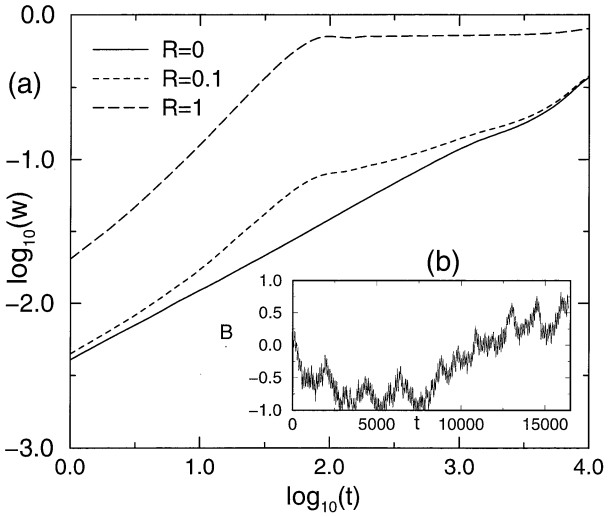

Fig. 3. (a) The effect of adding a periodic component to a noise signal with a Hurst exponent of 0.5. The width (Eqn. 4) was measured. R is the ratio of the peak-to-peak amplitudes of the periodic signal to the noise, and $t_p = 100$ is the period of the periodic component. The insert (b) shows the resulting pattern generated using $R = 0.1$.

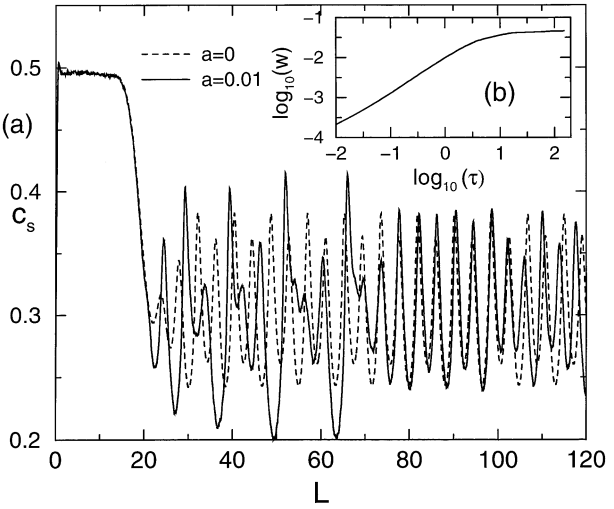

Fig. 4. (a) The solid composition c_s as a function of dimensionless distance from the core, $L = V_0 \int_0^t V(t')dt'/D$, for the plagioclase model, where $V_0 = V(c_0, T)$ is the steady state velocity. The dashed curve was generated using the parameters that were used to obtain Figure 3a in L'Heureux and Fowler (1996b), T=1600 K, K_D=0.34, c_i=0.5, and $\hat{c}$ = 0.3. The solid curve was generated using the same parameters, except that the molar fraction of anorthite at the end of the diffusion layer is equal to $0.3 + 0.01\,B(\tau)$, where $B(\tau)$ is Brownian noise limited between -1 and 1 (Fig. 1). The time step was 0.01. (b) The width w as a function of scaled time τ for the pattern shown in (a) with noise. The fit between $-2.0 < \log_{10}(\tau) < 0.5$ gives $H = 0.85$.

$$\frac{\partial c}{\partial t} = D\frac{\partial^2 c}{\partial x^2} + V\frac{\partial c}{\partial x} - \Gamma(c - \hat{c}). \tag{13}$$

In this model, the solute partitioning law is

$$c_s(t) = Kc(0,t), \tag{14}$$

and the boundary equations are $c(b, t) = \hat{c}$, where $\hat{c}$ is the constant concentration at the end of the diffusion layer and

$$D\,\frac{\partial c}{\partial x}\Big|_{x=0} + [c(0,t) - c_s(t)]V = 0. \tag{15}$$

In these equations, $c = c(x, t)$ is the concentration (molar fraction of anorthite) at a distance x from the crystal interface at time t, c_s is the concentration inside the solid, V is the growth velocity, K is the partition coefficient, D is the diffusion constant in the melt (the diffusion coefficient is assumed to be zero in the solid) and Γ is the input flow rate per unit volume. Here, $c(b,t)$ is the concentration at the boundary layer, far from the solid-fluid interface. The initial condition is $c(x,0)=c_i$. The $K = 1.5$ and $K = 0.55$ cases were studied. A nonoscillatory solution was found for $K = 1.5$, and an oscillatory solution was found for $K = 0.55$. A value of 0.55 is realistic for the partition coefficient K for An_{33} (33% anorthite) and $K = 1.5$ is realistic for An_{50} if the plagioclase grows from a typical basaltic melt. The growth velocity $V(c(0, t), T)$ was estimated (L'Heureux, 1993) by fitting the laboratory measurements of Kirkpatrick et al. (1979) to the Calvert-Uhlmann growth model (Calvert and Uhlmann, 1972). In some parts of the parameter space, the oscillatory solution was found to be chaotic. All parameters in the model can be estimated from experimental and geological data (L'Heureux and Fowler, 1994). In more recent studies (L'Heureux and Fowler, 1996a,b; L'Heureux, 1997) the growth equation was changed to

$$\frac{\partial c}{\partial t} = D\frac{\partial^2 c}{\partial x^2} + V\frac{\partial c}{\partial x}, \tag{16}$$

to represent growth in a closed system, and the solute partitioning law

$$c_s(t) = \frac{K_D B c(0,t)}{A + (K_D - 1)c(0,t)} \tag{17}$$

derived by Lasaga (1982) was used, where K_D is the partition coefficient and A and B are constants. Eqn. 13 is similar to Eqn. 16 because a very small value was chosen for Γ in the earlier work of L'Heureux and Fowler. The qualitative behavior of this model is the same as that of the earlier plagioclase model. The model can generate steady state, periodic and chaotic patterns, depending on the parameters. The steady state melt concentration at the interface is $c_0 = \hat{c}A/(K_D B - (K_D - 1)\hat{c})$. A period doubling route to chaos was observed in the more refined model (L'Heureux and Fowler, 1996a,b; L'Heureux, 1997) but not in the version of L'Heureux (1993) and L'Heureux and Fowler (1994). A Hopf bifurcation characterizes the transition from steady state to oscillatory solutions in both versions of the model. In the work of L'Heureux (1997), the effects of cooling on crystallization were studied.

Noise was added to this model (Eqns. 16 and 17) by replacing the fixed concentration boundary condition by $\hat{c}(t) = \hat{c}(0) + aB(t)$, where a is the amplitude of the noise and $B(t)$ is Brownian motion limited between -1 and 1. The main reason for using Brownian noise as an input, instead of white noise, is that in the case of Brownian noise, the concentration differences are small in the limit of a small time difference. Figure 4a shows results from two simulations with the same parameters, one with zero noise and the other with a noise amplitude of $a = 0.01$. The integration method was the same as that used by

L'Heureux (1993) and by L'Heureux and Fowler in subsequent articles. In this model, small amounts of noise can lead to large changes in the zoning pattern. Figure 4b, shows the width (Eqn. 4) calculated for the pattern with noise (the width function $w(l)$ for the pattern without noise was almost the same). The range over which apparent power law scaling was found is not large enough to establish fractal concentration profiles. If white noise is used instead of Brownian noise, the resulting pattern is very irregular on small scales. The Lyapunov exponent λ was measured (Fig. 5b) for the zoning pattern in Figure 5a by using Eqn. 11. A value of $\lambda = 0.95 \pm 0.10$ was measured by averaging over the ϵ values (neighborhood sizes) 0.0001, 0.001 and 0.01. This high value of the exponent shows that, with these parameters, the plagioclase model is very sensitive to noise. Using interference imaging techniques, Pearce and Kolisnik (1990) showed that plagioclase zoning is often discontinuous. This suggests that plagioclase growth is a highly non-linear phenomenon if the discontinuities are not caused by dissolution. Simulations were run with a variety of parameters, and synchronization was not found.

2.4 Calcite Model

Wang and Merino (1992) proposed a model for oscillatory zoning in calcite, based on growth inhibition by cations such as Mn^{2+}, Fe^{2+} and Zn^{2+} (Meyer, 1984). Depending on the values of the parameters, the patterns are periodic with a constant amplitude, periodic with decreasing amplitude or the solutions of the equations evolve monotonically toward a stable form corresponding to constant concentration profiles. The patterns are never chaotic. The precipitation of calcite is governed by the chemical reaction

$$Ca^{2+} + HCO_3^- \rightarrow CaCO_3(\text{calcite}) + H^+.$$

The forward reaction rate R of this chemical reaction is $R = kc^0_{Ca^{2+}} \cdot c^0_{HCO_3^-}$, where c_i^0 is the concentration of species i next to the crystal surface and k is a constant. When calcite grows, H^+ is released and accumulates at the surface if the reaction rate is fast compared with the diffusion rate. The attachment of species to the crystal surface may accelerate or inhibit the rate of mineral growth or dissolution (Helgeson et al., 1984). The surface charge of calcite depends on the pH. The reaction scheme coupled with diffusive transport leads to a feedback mechanism that can produce oscillatory zoning. The dimensionless concentrations u and v are defined as

$$u = c^0_{Ca^{2+}}/c^\infty_{Ca^{2+}} \tag{18}$$

and

$$v = (c^0_{H_2CO_3} - c^\infty_{H_2CO_3})/c^\infty_{H_2CO_3}, \tag{19}$$

where c^∞ is the concentration outside the boundary layer. The reaction rate constant k was assumed to be a quadratic function of the scaled H^+ concentration, defined as $z = (c^0_{H_+} - c^\infty_{H_+})/c^\infty_{H_+}$:

$$k = \alpha(1 + \beta_1 z + \beta_2 z^2), \tag{20}$$

where α, β_1 and β_2 are reaction rate constants. The equations

$$\frac{du}{d\tau} = 1 - u - \lambda(1 + \beta_1 v + \beta_2 v^2)u \tag{21}$$

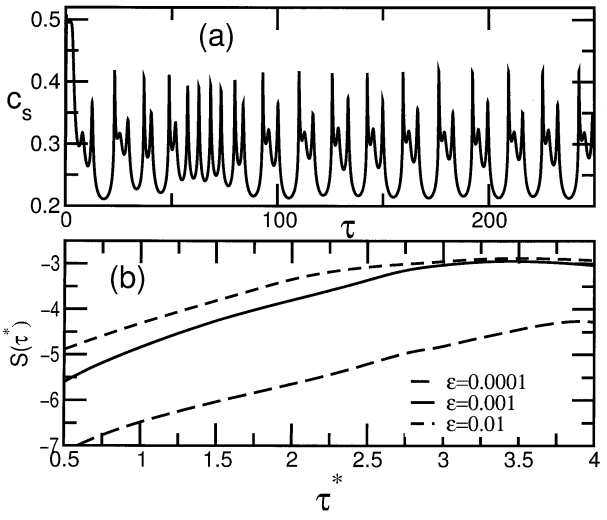

Fig. 5. (a) The solid composition c_s as function of dimensionless time τ obtained from the plagioclase model. The parameters are T=1600 K, $c_i = 0.5$, $\hat{c} = 0.3$, and $K_D = 0.31$. This is the same figure as Figure 3b in L'Heureux (1996b), except that the abscissa is τ instead of length. (b) Calculation of the Lyapunov exponent λ. $S(\tau^*)$ was calculated using Eqn. 11 for a simulation with the parameters used to obtain part (a). The effective Lyapunov exponent is the slope of the curve. The $250 < \tau < 2500$ region (not shown in (a)) was used to calculate $S(\tau^*)$. The initial neighborhood sizes ϵ were 0.0001, 0.001, and 0.01, respectively. The time step was 5×10^{-3}.

and

$$\theta \frac{dv}{d\tau} = -v + \gamma\lambda(1 + \beta_1 v + \beta_2 v^2)u, \tag{22}$$

were used to describe the chemical kinetics and material transport processes, the detail of the derivation can be found in Wang and Merino (1992). In these equations,

$$\lambda = \frac{\alpha c^\infty_{HCO_3^-} L}{D_{Ca^{2+}}}, \tag{23}$$

$$\theta = \frac{D_{Ca^{2+}}}{D_{H_2CO_3}}, \tag{24}$$

$$\gamma = \frac{D_{Ca^{2+}} c^\infty_{Ca^{2+}}}{D_{H_2CO_3} c^\infty_{H_2CO_3}}, \tag{25}$$

and $\tau = t/T$ is the dimensionless time, where $T = L/(2D_{Ca^{2+}})$ (L is the width of the diffusion layer), c is the concentration, and D is the diffusivity. Figure 6 shows some patterns generated by this model. The fourth order Runge-Kutta integration method was used to obtain numerical solutions for this model as well as for the garnet and Wang and Wu models described later in this article. The time step was fixed and equal to the time increment in the noise signal. The parameter θ was varied, but all the other parameters were kept constant. Depending on the value selected for θ, oscillations with constant amplitude and oscillations with decreasing amplitude were found. Bryxina and Sheplev (1997) found the steady states of this model, and located the boundaries between the different regions. None of the parameters, except the diffusivities and L, are known ex-

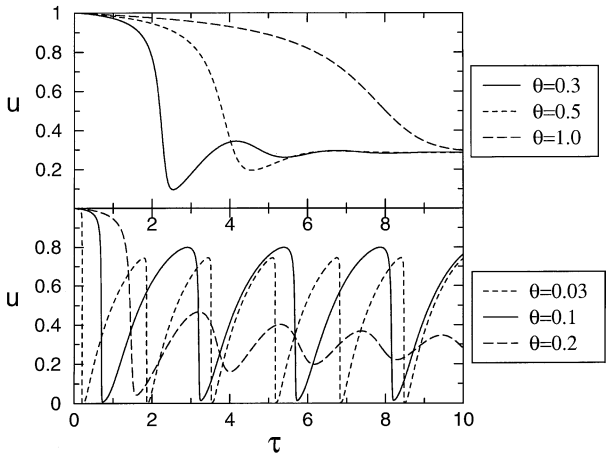

Fig. 6. The effect of changing the parameter θ in the calcite model. The curves show the scaled concentration (u) of Ca^{2+} as a function of the scaled time τ. The other parameters are $\gamma = 2$, $\lambda = 0.01$, $\beta_1 = 0$ and $\beta_2 = 80$. These parameters were used by Wang and Merino (1992) to generate Figure 6a in their paper, except that in our simulations $\gamma = 2$ is constant. When θ is increased, the amplitude of the oscillation at first increases, but does not decay with time. When $\theta > 0.17$ the amplitude decreases with increasing time.

perimentally. This makes meaningful comparison between simulations and geological samples difficult.

2.4.1. Adding noise

There are several ways to introduce noise to this model, but probably the best way is to add fluctuations to the calcium ion concentration at the end of the diffusion layer. This was done by changing $c^{\infty}_{Ca^{2+}}$ to

$$c^{\infty}_{Ca^{2+}}(t) = c'_{Ca^{2+}} + aB(t). \tag{26}$$

where $c'_{Ca^{2+}}$ is a constant, a is the amplitude of the noise and $B(t)$ is Brownian noise limited between -1 and 1, starting with $B(0) = 0$. By inserting Eqn. 26 into Wang and Merino's (1992) original equations, the equation

$$\frac{dc^0}{d\tau} = c^{\infty} - c^0 - \lambda(1 + \beta_1 v + \beta_2 v^2)c^0 - \frac{dc^{\infty}}{d\tau} \tag{27}$$

is obtained. Because $c^{\infty}_{Ca^{2+}}$ is included in the expression for γ (Eqn. 25), Eqn. 22 must be changed to

$$\theta \frac{dv}{d\tau} = -v + \gamma'\lambda(1 + \beta_1 v + \beta_2 v^2)c^0, \tag{28}$$

where

$$\gamma' = \frac{D_{Ca^{2+}}}{D_{H_2CO_3}c^{\infty}_{H_2CO_3}}. \tag{29}$$

Figure 7 shows some of the effects of noise on this model. As the amplitude a of the noise is increased, the period of oscillation increases, and the patterns have a more "noisy" appearance. The amplitude of oscillation remains approximately constant as a is increased from 0 to 0.3. Figure 8 shows the power spectra (Press et al., 1992) of three of the patterns in Figure 7. The power spectrum of the perfectly periodic pattern ($a = 0.0$) has a large peak at the frequency of oscillation, and at higher harmonics (integer multipliers of the frequency of oscillation). The peaks of the perfectly periodic pattern have a finite width, because of finite size effects, and longer simulations lead to sharper peaks. As a increases, the peaks becomes broader and eventually disappear. This is a general effect of adding noise to a model that generates periodic or quasi-periodic patterns when there is no noise. If two systems start with different values of $c'_{Ca^{2+}}$, but the other parameters are the same and they are subjected to the same noise, they never synchronize.

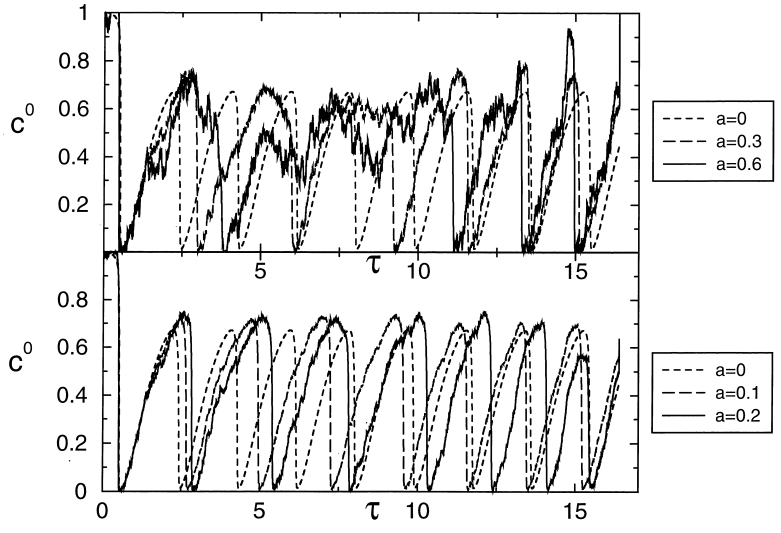

Fig. 7. The effect of noise on the Wang and Merino calcite growth model. The curves show the concentration c^0 of Ca^{2+} as a function of the scaled time τ. The noise amplitude a was increased from 0 to 0.6. The other parameters were $\gamma = 2$, $\beta_1 = 70$, $\beta_2 = 100$, $\theta = 0.1$, $\lambda = 0.01$, and $c'_{Ca^{2+}} = 1.0$. These parameters were used in Figure 2 of Wang and Merino (1992).

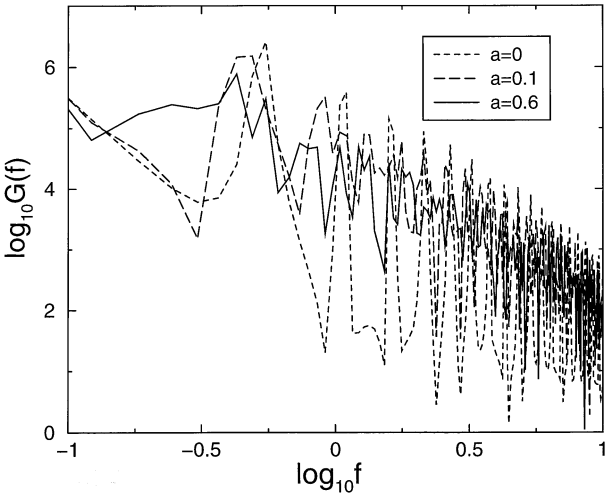

Fig. 8. The power spectra of three patterns in Figure 7, with $a = 0$, 0.1, and 0.6 respectively.

2.5. Garnet Model

Jamtveit (1991) presented a model for oscillatory zoning of grossular-andradite (grandite) garnets and found oscillatory and chaotic solutions. The model is based on an observed miscibility gap in grandite garnets. A symmetric potential G of the form

$$G(u) = u^4/4 - u^2/2 \tag{30}$$

was used to describe the excess free energy of mixing. Here, u is a dimensionless composition variable. The minima of the potential are at $u = \pm 1$. The force acting on the system in the potential field is the gradient of $G(u)$,

$$\ddot{u} = -\nabla G(u). \tag{31}$$

Inserting Eqn. 30 into Eqn. 31 gives

$$\ddot{u} - u + u^3 = 0. \tag{32}$$

A dissipative term and periodic forcing of the system were added, leading to the equation

$$\ddot{u} + \sigma\dot{u} - u + u^3 = \gamma cos(wt), \tag{33}$$

where σ is a constant controlling the degree of dissipation in the system. There is no transport in the model, since there are no spatial variables. This equation is similar to the Duffing equation, one of the most common models of nonlinear oscillatory systems. The general Duffing equation (Zeni and Gallas, 1995) is

$$\ddot{x} + a\dot{x} + \alpha x + \beta x^2 + x^3 = bf(t), \tag{34}$$

where $f(t)$ is a periodic function driving the system, and a, α, b, and β are parameters. The solutions to Eqns. 33 and 34 can be chaotic, depending on the parameters. A minimum criteria for chaos (Guckenheimer and Holmes, 1983) is that $\gamma > (4\sigma \cosh (\pi\omega/2)/3\sqrt{2}\pi\omega)$. If $\omega = 1$, this equation reduces to $\gamma > 0.753\sigma$. Figure 9 shows the Lyapunov exponent, λ, (Eqn. 8), calculated by using the method described by Kantz (1994) (Eqn. 11), as a function of σ and λ. When $\lambda > 0$, there is chaos. A bifurcation can be seen in this plot. The Lyapunov exponent is an irregular function, $\lambda(\sigma,\gamma)$, of σ and γ. A similar plot was shown by Zeni and Gallas (1995) for the equation $\ddot{x} + a\dot{x} + x^3 = bcos(t)$, and it was found that windows of periodicity appear in a quite organized way between regions in which $\lambda(a,b)$ is an irregular function of a and b. Lansbury et al. (1992) studied the phase portrait of Eqn. 33, focusing on the loss of stability of motion confined to a single well. Two distinct bifurcation scenarios were described in which the basin boundaries of the attractor are fractal.

Noise can be added by changing Eqn. 33 to

$$\ddot{u} + \sigma\dot{u} - u + u^3 = aB(t) + \gamma\cos(\omega t) \tag{35}$$

Figure 10a shows synchronization in the solutions of Eqn. 35. There are two curves that lie (almost) exactly on top of each other, after a certain time, if Brownian noise with an amplitude of 0.10 was added. One curve starts at $u=0$, and the other at $u = 1$. Figure 10b shows the start of the synchronization. At a later stage, shown in Fig. 10c, the two patterns are no longer synchronized, although the difference between the patterns in Figure 11b was less than 10^{-10}. Finally, the patterns (almost) synchronize in Figure 10d. The patterns are nearly synchronized when the value of u corresponds to regions near the minima of the potential wells, and are desynchronized in between. Desynchronization can also occur in other dynamical systems (Pecora, 1998; Heagy et al., 1995). Leung (1998) examined the time needed for synchronization of the solutions of two coupled van der Pol oscillators. A kind of phase transition at which the transient dynamics changed qualitatively as the coupling constant was varied, was discovered. In addition to the asymptotic synchronization, a transient synchronization that occurs only momentarily was found. The influence of noise on the system depends on the location in phase space for the Duffing equation with Gaussian white noise (Jaeger and Kantz, 1997).

Stochastic resonance is the amplification of a weak signal by noise in a nonlinear system (Gammaitoni et al., 1998). Stochastic resonance can probably occur in oscillatory zoned crystals, because the required three basic ingredients for producing stochastic resonance often are present. These three ingredients are (1) an energetic activation barrier, (2) a weak coherent input (for instance, a periodic signal), and (3) a source of noise that is inherent to the system, or that is superimposed on the coherent input. There are however exceptions to the second requirement, since stochastic resonance also can occur in autonomous systems. An example of autonomous stochastic resonance is noise-induced firing of neurons without external forcing (Longtin, 1997). The regions of synchronization (Fig. 10b,d) are examples of stochastic resonance, the periodic signal is here amplified by noise. Gammaitoni et al. (1998) found that if Gaussian noise instead of Brownian noise is added to Eqn. 33 the behavior is similar to that shown in Figure 2c.

Nearby crystals may not experience exactly the same noise. For example, local noise may be superimposed on the noise originating far away from the crystal, or the effects of the noise originating far away may be propagated to the growing crystal in different ways, because of heterogeneities in the environment. Simulations were run with the same Brownian noise, and a different Gaussian noise signal (all with the same amplitude)

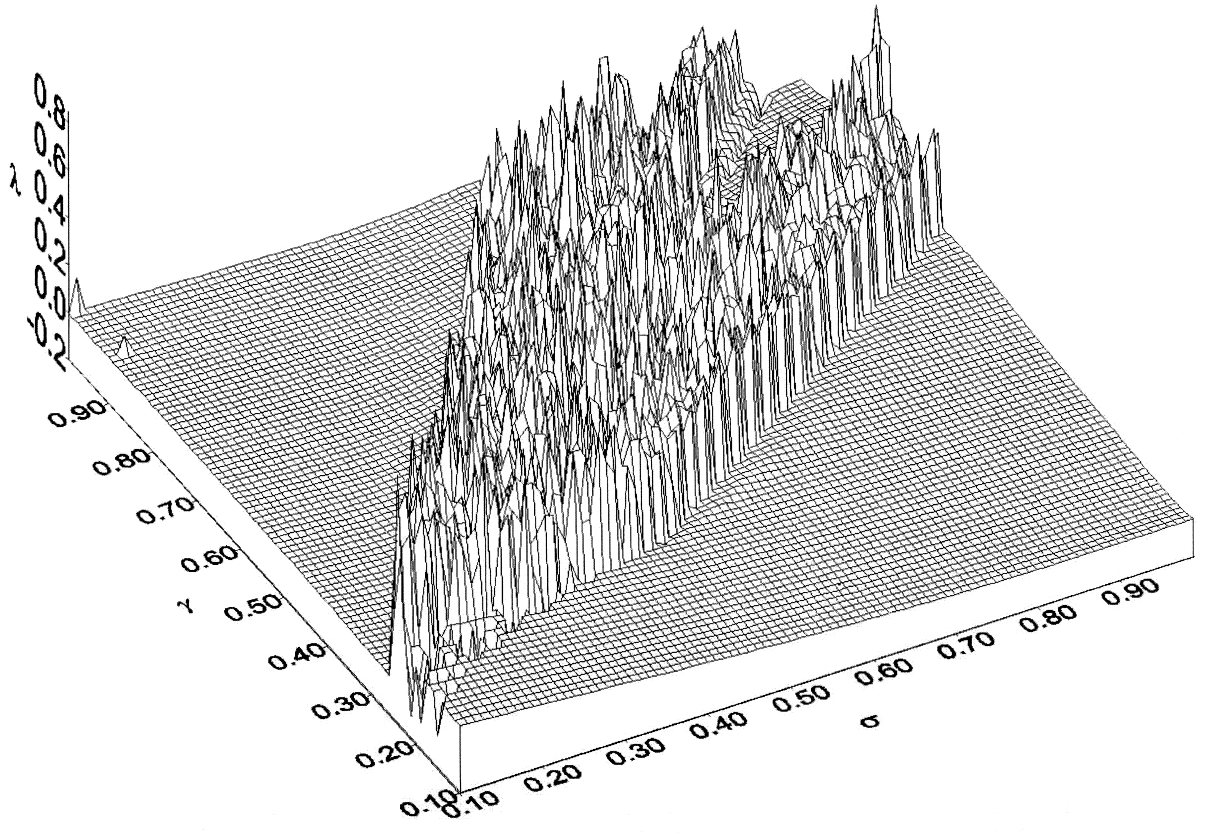

Fig. 9. The Lyapunov exponent λ as a function of σ and γ when $\omega = 1$ for the garnet model (the simplified Duffing equation). The method described by Kantz (1994) was used to measure λ.

were added. The synchronization behavior was not sensitive to small amplitude Gaussian noise. For instance, a simulation with Gaussian noise with a standard deviation of 0.03 superimposed on the simulation in Figure 10 ($\sigma = 0.30$, $\gamma = 0.30$, $\omega = 1$ and $a = 0.10$) gave patterns that differed less than 0.001 in $u(t)$. In the regions of synchronization, there are oscillations that have the same frequency and approximately the same phase as the $\cos(\omega t)$ term, but with amplitudes that vary somewhat with time t. When the Brownian noise has low values, the system fluctuates symmetrically about -1, and when the Brownian noise has high values, it fluctuates about $+1$, because the system is constantly driven away from $u = 0$. Because the Gaussian noise has an average of zero, it has only a minor effect and does not prevent the system from being kept in synchronization with the $\cos(\omega t)$ term, as long as the Brownian term has either low or high values. Increasing the amplitude of the Gaussian noise leads to larger differences in the amplitudes of oscillations, but the two signals still have the same phase in the regions of synchronization. Finally, when the amplitude of the Gaussian noise is very large (above 0.4) the synchronization is destroyed.

2.6. The Wang and Wu Model

Wang and Wu (1995) presented a simple, nonequilibrium nonlinear dynamic model to describe solid solution growth in a melt. They derived the equation

$$f = 1/((1 + (\beta/X^S))(1 - X^S)\exp(-W/RT)(1 - 2f)), \quad (36)$$

for the mole fraction f of a component in the solid as a function of the mole fraction X^S of the same component in the fluid phase, where W is the total interchange energy, R is the gas constant, T is the temperature and $\beta = k_B/k_A$, with k_A and k_B representing the overall crystallization rate constants of components A and B. This equation is based on a solution model with an interchange energy W and no excess entropy. If $W/RT < -2$, f is a multi-valued function of X^S. The model is completed by a mass–balance equation. The growth equation with zero diffusion constant is

$$dX^S/d\tau = (X^\infty - f)V, \quad (37)$$

where V is the dimensionless velocity, τ is the dimensionless time and X^∞ is the starting concentration. Only the unrealistic zero and infinite diffusion coefficient cases were treated by Wang and Wu (1995). The model always leads to periodic patterns with a constant amplitude if $W/RT < -2$.

One way of investigating the effects of adding noise to this model is to replace the constant mole fraction X^S by a fluctuating function $X^S(t)$ and examine the output $f(t)$ from Eqn. 36. Figure 11a shows the input noise $X^S(t)$, limited between 0 and 1, and Figure 11b shows the output $f(t)$. There are large jumps in the composition record, $f(t)$, whenever the input X^S reaches certain threshold values. This behavior is analogous to that

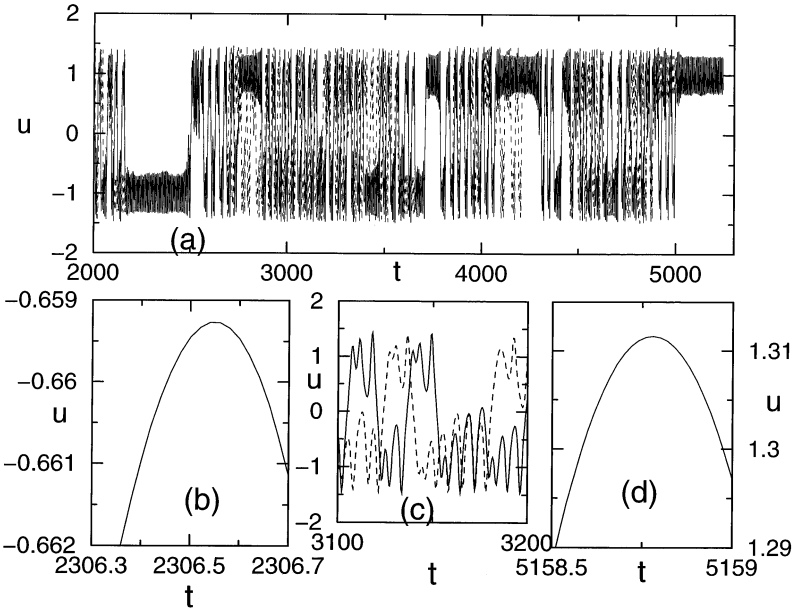

Fig. 10. This figure shows synchronization in the garnet model. The parameters were $\sigma = 0.30$, $\gamma = 0.30$, $\omega = 1$, and $a = 0.10$. One curve was started with $u = 0$ (dashed line) and the other with $u = 1$ (solid line). (a) A large part of the zonation pattern in which parts (b), (c), and (d) are included. (b) A detailed plot of a part in which the two curves are (almost) synchronized. (c) A later stage, in which the two patterns are no longer synchronized. Part (d) shows that at a still later stage, the two patterns are (almost) synchronized again. In (b) and (d) the two curves lie on top of each other so that only one curve can be seen.

shown in Figure 2. We believe that such noise-induced transitions are common during the growth of strongly non-ideal solid solution minerals in open systems subject to a noisy environment. Large compositional jumps may correspond to sudden events like fracturing and associated fluid flow in a hydrothermal system, or sudden decompression of a magmatic system (Holten et al., 1997).

Noise can also be added by letting

$$X^{\infty} = X^0 + aB(\tau), \tag{38}$$

where X^0 is the new starting concentration, a is the amplitude of the noise and $B(\tau)$ is Brownian motion limited between –1 and 1. Figure 12 shows a pattern obtained by integrating Eqns. 36 and 37 and patterns generated using added noise (Eqn. 38) with amplitudes of $a = 0.1$ and $a = 0.5$. The pattern with $a = 0.1$ is similar to the $a = 0$ curve, except that the period of oscillation fluctuates by up to 10%. The pattern with maximum noise $a = 0.5$ (to avoid negative concentrations) is heavily distorted. This model does not show synchronization since it is not chaotic.

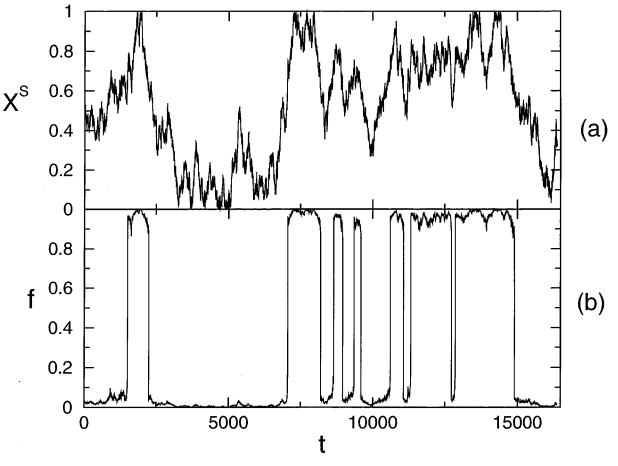

Fig. 11. The effect of noise on Wang and Wu's equation (Wang and Wu, 1995) for the solid composition f as a function of the fluid composition X^s (Eqn. 36). (a) The curse $X^s(t)$ used as an input. (b) The composition $f(t)$ calculated using Eqn. 36 (for every time step, the concentration f was calculated from X^s using Eqn. 36.

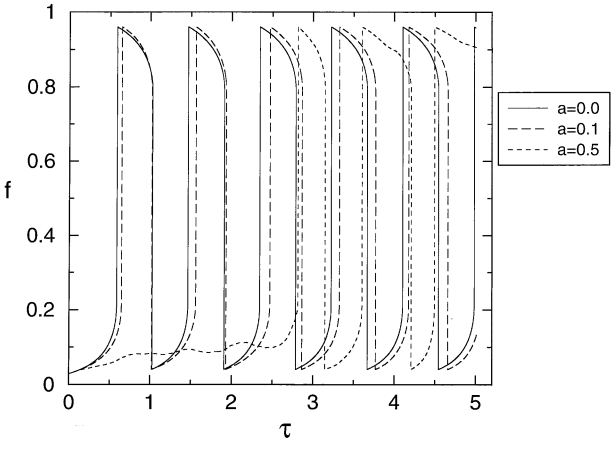

Fig. 12. Results from adding noise to the Wang and Wu model, using Eqn. 38. The curve with $a = 0$ corresponds to Figure 5 in Wang and Wu (1995) with parameters $\beta = 2$, $W/RT = -3$, and $V = 1$. The other two curves were obtained using the same parameters except that $a = 0.1$ and 0.5 respectively.

3. DISCUSSION

Recent work has shown that oscillatory intracrystalline zonation is more common than hitherto thought in a variety of geological systems. It is likely that despite the influence of the external environment, some of the observed pattern arise because of nonlinear processes associated with the crystal growth itself. This is particularly the case for oscillatory zoned magmatic crystals for which the lack of intracrystalline correlations in the zonation patterns argue for a self-organized origin of the patterns. In such systems attempts to infer the growth mechanism from the observed zonation pattern has turned out to be a nontrivial task, and the situation is even more complicated for hydrothermally grown crystals. There is no guarantee that these inverse problems have unique solutions, but it is often possible to put important constraints on the processes that might lead to a particular pattern. Noise is a ubiquitous feature of many natural systems, and many nonlinear systems are sensitive to noise. Consequently, it is to be expected that many natural patterns, including mineral zonation patterns, are significantly affected by noise and system heterogeneities. The extent to which processes leading to mineral zonation can be deduced from quantitative characterization of mineral zonation patterns depends on the degree to which the effects of noise and heterogeneities are understood. In the case of crystal growth, fast compositional changes at the outer margin of the diffusion layer may render deterministic models for self-organization inadequate. Noise need not be restricted to fluctuations in concentration of the crystal forming components, but can also be fluctuations in other intensive variables such as oxygen fugacity, pH, and temperature. For example, the composition of grandite garnets is expected to be sensitive to changes in all these variables (Jamtveit et al., 1995). In hydrothermal systems in particular, environmental fluctuations in both composition and temperature may easily be envisaged as a result of changes in fluid flow rates and flow paths, even on a short time scale (Jamtveit, 1999). The models studied here have different degrees of sensitivity to noise. Noise disturbs the period of oscillations in the calcite model. Low amplitude noise has a large impact on the plagioclase growth model, so that two crystals experiencing slightly different conditions would develop qualitatively different zoning patterns.

It has been claimed that one way of distinguishing self-organization from external fluctuations as the main cause for mineral zoning, is to study neighboring mineral grains. If these mineral grains all show similar zoning, it has been concluded that external fluctuations are the probable cause of mineral zoning. The lack of such intracrystalline correlation has been taken as an indication of internal nonlinear behavior. The above analysis shows that this is not always a reliable criterion, because small amounts of noise can lead to synchronization, as illustrated by the results obtained by adding noise to the garnet model. In this situation, the external noise has a controlling influence on the pattern details, but pattern formation would not occur without the internal autonomous nonlinear dynamics of the system. The addition of noise to published models generates patterns that appear to be more realistic than those obtained without noise. To the best of our knowledge, crystals that show perfectly periodic zoning patterns have not been found in geological samples. Noise can drive the system from one equilibrium state to another. Guillouzic and L'Heureux (1997) derived an equation for the transition rate from one deterministic attractor to another. This rate depends on the amplitude and nature of the noise as well as the system itself.

Complex mineral zonation patterns can be statistically characterized either as a purely geometrical object, or as a time series. The Lyapunov exponent measurements described above may give valuable insight into the dynamics of the processes responsible for generating the pattern. Halden (1996) measured the Lyapunov exponent (λ) for zircon and apatite cathodoluminence zonation patterns and found that $0.0011 < \lambda < 0.0149$, which means that the patterns are weakly chaotic. This result contrasts with the conclusions reached by Holten et al. (1997), who found no indication for underlying chaos in their analysis of zonation patterns from samples of garnet, vesuvianite and plagioclase. The plagioclase and garnet models have positive Lyapunov exponents in parts of the parameter space, while the calcite and Wang and Wu (1995) models always have negative Lyapunov exponents, since only periodic (or monotonic) patterns are possible.

Zonation patterns can be characterized by fractal analysis or by any other relevant statistical method. In practice, fractal geometry is indicated by straight lines in log–log plots. However, the range of scaling obtained in this manner may be insufficient to reliably establish fractal behavior, and linear behavior over a short range on a log–log scale is often misleading. If a periodic component is added to a fractal, an incorrect effective Hurst exponent can be measured (see Fig. 2). Brownian processes cannot model large jumps in composition, but other fractal models can be used. The discrepancy between complicated natural zonation patterns, and deterministic models for self-organizing oscillatory patterns is part of the motivation for investigating models that couple external fluctuations and the resulting zonation pattern, by adding noise to four published models for oscillatory zoning of minerals.

A set of differential equations or an algorithmic model provides, at best, an approximate description of the behavior of a real system. Even if a theoretical model is accurate, there are often large uncertainties concerning the conditions under which the pattern was formed and the associated model parameters. Data analysis is also an important source of uncertainty. For example the concentration profiles obtained from mineral zonation patterns usually contain far too few points to allow an accurate determination of a Hurst exponent to be carried out or for the dimensionality of an underlying nonlinear process to be determined. In this article, we have focused on another source of uncertainty—the coupling between the intrinsic nonlinear dynamics of a system and fluctuation in its environment. It is apparent that the interpretation of zoning patterns in terms of physico–chemical processes and geological conditions still presents a difficult challenge. A sound understanding of all of the processes involved in the formation of zoning patterns and the interactions between them is required if they are to be used to reliably interpret the geological condition of their formation.

Acknowledgments—The authors thank Ivan L'Heureux for valuable discussions and assistance with programming, Massimo Cortini for testing chaotic behavior, Tao Sun for assistance with programming, and Enrique Merino for a thorough review that helped to clarify the article. This work was supported by The Norwegian Research Council through

the "Fluid Rock Interaction" strategic University program (grants 440.96/006 and 440.56/007) and through a grant of Supercomputer time.

REFERENCES

Bryxina N. A. and Sheplev V. S. (1997) Oscillatory zoning in calcite growing from an aqueous solution (in Russian). *Mathematical Modeling* **9,** 32–38.

Calvert P. D. and Uhlmann D. R. (1972) Surface nucleation growth theory for large and small crystal cases and the significance of transient nucleation. *J. Cryst. Growth* **12,** 291–296.

Gammaitoni L., Hänggi P., Jung P., and Marchesoni F. (1998) Stochastic resonance. *Rev. Modern Physics* **70,** 223–287.

Guckenheimer J. and Holmes P. (1983) *Nonlinear Oscillations, Dynamical Systems, and Bifurcations of Vector Fields*. Springer-Verlag.

Guillouzic S. and L'Heureux I. (1997) Kinetics of dichotomous noise-induced transitions in a multistable multivariable system. *Phys. Rev. E* **55,** 5060–5072.

Gutiérrez J. M. and Iglesias A. (1998) Synchronizing chaotic systems with positive conditional Lyapunov exponents by using convex combinations of the drive and response systems. *Phys. Lett. A* **239,** 174–180.

Halden N. M. (1996) Determination of Lyapunov exponents to characterize the oscillatory distribution of trace elements in minerals. *Can. Mineral.* **34,** 1127–1135.

Halden N. M. and Hawthorne F. C. (1993) The fractal geometry of oscillatory zoning in crystals: Application to zircon. *Am. Mineral.* **78,** 1113–1116.

Hasler M., Maistrenko Y., and Popovych O. (1998) Simple example of partial synchronization of chaotic systems. *Phys. Rev. E* **58,** 6843–6846.

Heagy J. F., Carroll T. L., and Pecora L. M. (1995) Desynchronization by periodic orbits. *Phys. Rev. E* **52,** R1253–R1256.

Helgeson H. C., Murphy W. M., and Aagaard P. (1984) Thermodynamic and kinetic constraints on reaction rates among minerals and aqueous solutions. II. Rate constants, effective surface area, and the hydrolysis of feldspar. *Geochim. Cosmochim. Acta* **48,** 2405–2432.

Holten T., Jamtveit B., Meakin P., Cortini M., Blundy J., and Austrheim H. (1997) Statistical characteristics and origin of oscillatory zoning in crystals. *Am. Mineral.* **82,** 596–606.

Jaeger L. and Kantz H. (1997) Homoclinic tangencies and non-normal Jacobians. Effects of noise in nonhyperbolic chaotic systems. *Physica D* **105,** 79–96.

Jamtveit B. (1991) Oscillatory zonation patterns in hydrothermal grossular-andradite garnet: Nonlinear dynamics in regions of immiscibility. *Am. Mineral* **76,** 1319–1327.

Jamtveit B., Ragnarsdottir K. V., and Wood B. J. (1995) On the origin of zoned grossular-andradite garnets in hydrothermal systems. *Eur. J. Mineral* **7,** 1399–1410.

Jamtveit B. (1999) Crystal growth and intracrystalline zonation patterns in hydrothermal environments. In *Growth, dissolution and pattern formation in geosystems* (eds. B. Jamtveit and P. Meakin), pp. 65–84. Kluwer Academic Publishers.

Jamtveit B. and Meakin P. (1999) *Growth, dissolution and pattern formation in geosystems*. Kluwer Academic Publishers.

Kantz H. (1994) A robust method to estimate the maximal Lyapunov exponent of a time series. *Physics Lett. A* **185,** 77–87.

Kirkpatrick R. J., Klein L., Uhlmann D. R., and Hays J. F. (1979) Rates and processes of crystal growth in the system anorthite-albite. *J. Geophys. Res.* **84,** 3671–3676.

Lansbury A. N., Thompson J. M. T., and Stewart H. B. (1992) Basin erosion in the thin well Duffing oscillator: Two distinct bifurcation scenarios. *Int. J. Bif. Chaos* **2,** 505–532.

Lasaga A. C. (1982) Toward a master equation in crystal growth. *Am. J. Sci.* **282,** 1264–1288.

Leung H. K. (1998) Critical slowing down in synchronizing nonlinear oscillators. *Phys. Rev. E* **58,** 5704–5709.

L'Heureux I. (1993) Oscillatory zoning in crystal growth: A constitutional undercooling mechanism. *Phys. Rev. E* **48,** 4460–4469.

L'Heureux I. (1997) Oscillatory zoning in plagioclase: Thermal effects. *Physica A* **239,** 137–146.

L'Heureux I. and Fowler A. D. (1994) A nonlinear dynamical model of oscillatory zoning in plagioclase. *Amer. Mineral.* **79,** 885–891.

L'Heureux I. and Fowler A. D. (1996a) Isothermal constitutive undercooling as a model for oscillatory zoning in plagioclase. *Can. Mineral.* **34,** 1137–1147.

L'Heureux I. and Fowler A. D. (1996b) Dynamical model of oscillatory zoning in plagioclase with nonlinear partition relation. *Geophys. Res. Lett.* **23,** 17–20.

Longtin A. (1997) Autonomous stochastic resonance in bursting neurons. *Phys. Rev. E* **55,** 868–876.

Lorenz E. N. (1963) Deterministic nonperiodic flow. *J. Atmos. Sci.* 20, 130–141.

Malescio G. (1996) Noise and synchronization in chaotic systems. *Phys. Rev. E* **53,** 6551–6554.

Mandelbrot B. (1982) *The fractal geometry of nature*. W. H. Freeman.

Maritan A. and Banavar J. R. (1994) Chaos, noise and synchronization. *Phys. Rev. Lett* **72,** 1451–1454.

Meakin P. (1998) *Fractals, scaling and growth far from equilibrium*. Cambridge University Press.

Merino E. (1984) Survey of geochemical self-patterning phenomena. In *Chemical Instabilities: Applications in Chemistry, Engineering, Geology, and Materials Science* (eds. G. Nicolis and F. Baras), pp. 305–328. NATO ASI series C, vol. 120.

Merino E. (1987) Textures of low-temperature self-organization. In *Geochemistry of the Earth's Surface* (eds. R. Rodriguez-Clemente and Y. Tardy), pp. 597–610. CSIC (Spain) and CNRS (France).

Meyer H. J. (1984) The influence of impurities on the growth rate of calcite. *J. Cryst. Growth* **66,** 639–646.

Ortoleva P. (1994) *Geochemical self-organization*. Oxford University Press.

Pearce T. H. (1994) Recent work on oscillatory zoning in plagioclase. In *Feldspars and their reactions* (ed. I. Parsons), pp. 313–349. NATO ASI.

Pearce T. H. and Kolisnik A. M. (1990) Observations of plagioclase zoning using interference imaging. *Earth Sci. Rev.* **29,** 9–26.

Pecora L. M. (1998) Synchronization condition and desynchronization patterns in coupled limit-cycle and chaotic systems. *Phys. Rev. E* **58,** 347–360.

Pecora L. M. and Carroll T. L. (1990) Synchronization in chaotic systems. *Phys. Rev. Lett.* **64,** 821–824.

Pikovsky A. S., Rosenblum M. G., Osipov G. V., and Kurths J. (1997) Phase synchronization of chaotic oscillators by external driving. *Physica D* **104,** 219–238.

Press W. H., Teukolsky S. A., Vetterling, W. T., and Flannery B. P. (1992) *Numerical recipes in C*. Cambridge University Press.

Putnis A., Fernandez–Diaz L., and Prieto M. (1992) Experimentally produced oscillatory zoning in plagioclase. *Nature* **358,** 743–745.

Reeder R. J., Fagioli R. O., and Meyers W. J. (1990) Oscillatory zoning of Mn in solution-grown calcite crystals. *Earth Sci. Rev.* **29,** 39–46.

Rosenstein M. T., Collins J. J., and De Luca C. J. (1993) A practical method for calculating largest Lyapunov exponents from small data sets. *Physica D* **65,** 117–134.

Scott S. K. (1991) *Chemical Chaos*. Clarendon Press.

Shore M. and Fowler A. D. (1996) Oscillatory zoning in minerals: A common phenomenon. *Can. Mineral.* **34,** 1111–1126.

Strogatz S. (1994) *Nonlinear dynamics and chaos*. Addison-Wesley.

Wang J.-H. and Wu J.-P. (1995) Oscillatory zonation of minerals and self-organization in silicate solid-solution systems: A new nonlinear dynamic model. *Eur. J. Mineral.* **7,** 1089–1100.

Wang Y. and Merino E. (1992) Dynamic model of oscillatory zoning of trace elements in calcite: Double layer, inhibition, and self-organization. *Geochem. Cosmochim. Acta* **56,** 587–596.

Zeni A. R. and Gallas J. A. C. (1995) Lyapunov exponents for a Duffing oscillator. *Physica D* **89,** 71–82.